



## STRUCTURAL PROPERTIES OF Ni<sup>2+</sup> VINYLPHOSPHONATE USING PM3 SEMI-EMPIRICAL ANALYSIS

Bianca MARANESCU,<sup>a</sup> Aurelia VISA,<sup>a</sup> Smaranda ILIESCU,<sup>a</sup> Adriana POPA,<sup>a</sup> Gheorghe ILIA,<sup>a,b</sup>  
Valentin MARANESCU,<sup>c</sup> Zeno SIMON<sup>a</sup> and Mircea MRACEC<sup>a,d,\*</sup>

<sup>a</sup> Institute of Chemistry Timișoara of the Roumanian Academy, 24 M. Viteazul Ave, Timișoara - 300223, Roumania

<sup>b</sup> West University, Faculty of Chemistry-Biology and Geography, 16 Pestalozzi Street, Timișoara - 300115, Roumania

<sup>c</sup> "Politehnica" University of Timișoara, Faculty of Electronics and Telecommunications, 2 Pârvan Ave.,  
Timișoara - 300223, Roumania

<sup>d</sup> "Aurel Vlaicu" University of Arad, 77 Revoluției Ave., Arad - 310130, Roumania

Received April 5, 2011

Research on phosphonates metal organic frameworks has attracted attention during the last two decades due to their fascinating network topology, structural flexibility and multiple special properties. The PM3 semi-empirical analyses of structural properties were made in order to predict the special properties (electrical properties, conductivity) and to compare the calculated and experimental geometric properties of the Ni<sup>2+</sup> vinylphosphonate metal organic framework. For this reason five octahedral models were calculated: with an increasing of number of Ni<sup>2+</sup> ions and phosphonates, three arising from constructed geometries and two from experimental X-ray data. For the PM3 semi-empirical results the calculated bond lengths are shorter than the experimental ones. The bond angles are comparable or higher and the torsion angles are comparable with the experimental results. The orbital distribution of the 3x3 Ni network (VP-9Ni) predict the electric proprieties of the Ni<sup>2+</sup> vinylphosphonate metal organic framework. The LUMO-HOMO energetic difference decreases from the TriVP-Ni to the VP-9Ni, structure which is the most realistic approximation for the real compound, from 8.68 reaching to a value of 4.99 eV. This difference explains the dielectric proprieties of VP-9Ni metal organic network, revealed also by current measurements into 0-20V DC voltage range. A mathematical relationship which demonstrates that for each Ni<sup>2+</sup> ion corresponds only one ligand to form a supramolecular network was deduced.

### INTRODUCTION

Most of metal organic frameworks exhibit a variety of open framework architectures.<sup>1-4</sup> These compounds received extensive research attention in recent years due to their potential applications in the areas of gas storage,<sup>5-7</sup> heterogeneous catalysis,<sup>8,9</sup> separation,<sup>10,11</sup> ion exchange,<sup>12</sup> magnetism,<sup>13</sup> sensors,<sup>14</sup> etc. Most networks are based on metal organic dicarboxylic derivatives that form a uniform structure with transition metal ions. Most of the metalphosphonates have a layered structure in which the metal centers are bridged by the phosphonate group, although a variety of 1D chain, 2D layer, and 3D network with micropores, among which the 2D layer is the most common structural type.<sup>15</sup>

An interesting class of metalphosphonates is the one that uses a phosphonic derivative containing a double bond. Thus, Ni<sup>2+</sup> vinylphosphonate was obtained by the reaction of NiSO<sub>4</sub>·7H<sub>2</sub>O vinyl phosphonic acid (VP) in echimolecular ratio and hydrothermal conditions.<sup>16-18</sup>

This compound was characterized by infrared spectroscopy (IR), atomic force microscopy (AFM), thermogravimetric analysis (TG) and differential scanning calorimetry (DSC). The thermogravimetric analysis for Ni<sup>2+</sup> vinylphosphonate metal organic framework indicated a loss process at 210-265°C which corresponds to the calculated mass loss for a water molecule coordinated to central Ni ion and the second weight loss at 340-500°C which correspond to the calculated mass loss for a vinylphosphonate (VP) molecule for each Ni<sup>2+</sup>.<sup>16-18</sup>

\* Corresponding author: [mracec@acad-icht.tm.edu.ro](mailto:mracec@acad-icht.tm.edu.ro)

In this paper the geometric properties (bond lengths, bond angles, torsion angles) and electronic properties (energetic levels, charges, heats of formation, ZPE,  $v_{\min}$ ,  $v_{\max}$ ) from semi-empirical PM3 calculation and X-ray experimental data were compared.

## METHODS

Gas phase equilibrium geometry of conformers was obtained by semi-empirical PM3-RHF calculations using the Polak-Ribiere conjugate gradient algorithm for geometry optimization.<sup>19,20</sup> Stop criteria were: SCF convergence of  $10^{-5}$  and RMS gradient of  $10^{-2}$  kcal/A·mol.<sup>20,21</sup> For the structures with  $\frac{1}{2}$  spin number we used half electron approximation. Calculations have been performed with HyperChem7.52 package.<sup>21</sup>

The  $v_{\min}$  (fundamental vibration) for all compounds is positive proving that the calculated geometries are stable structures, are stationary states but not transition states.

In preliminary electrical conductivity studies of  $\text{Ni}^{2+}$  vinylphosphonate, the compound was pressed between two 2 mm thickness, 2 cm diameter brass electrodes. After applying 10 minutes a 22 atm constant pressure, the final compound thickness was 1.6 mm, staying stiff between electrodes. The electrodes have been stimulated at a constant temperature of 25°C, with a 0-20V DC voltage range using a 1V step. A Keithley 2700 multimeter was connected in series with electrodes for current measurement. The settle time after each voltage step was chose to be 5s. For each measurement step the current range was small and close to maximum sensitivity of the tool, so the conclusion was that the compound behavior is similar to an insulator. As a reference, a 1mm insulating disc build of polyamide PA66 was inserted between electrodes and it was observed that currents values are into the same small range if identical DC voltage is applied.

## RESULTS AND DISCUSSION

A model can be built based on this information, where the vinylphosphonate ligand ( $\text{O}_3\text{P}-\text{CH}=\text{CH}_2$ )<sup>2-</sup> can form the complex  $[\text{Ni}(\text{VP})_3]^{4-}$ . In this model two negatively charged oxygen atoms from three VP ions form an octahedral coordination (Fig. 1a). For this structure, the oxygen atom double-bounded by phosphorus and

the vinyl radical do not help to build the network structure. The complex  $[\text{Ni}(\text{VP})_3]^{4-}$  contains no coordinated water molecule for each  $\text{Ni}^{2+}$  ion. According to the TG analysis results for each Ni ion a water molecule is chemically bound. Because that model does not correspond to the experimental results it will be used only as a comparison factor.

In a second possible model, all three oxygen atoms would coordinate the central ion. By complexation, an octahedral system can be realized using an elementary unit cell  $[\text{Ni}(\text{VP})_4 \cdot \text{H}_2\text{O}]^{6-}$  (Fig. 1b). The central ion is the  $\text{Ni}^{2+}$  ion and the ligands are 6 oxygen atoms (one belongs to the water molecule and 5 to the VP), in accordance with X-ray data.<sup>18</sup>

In the proposed elementary unit cell we suppose that two oxygen atoms from two phosphonate ions participate in the equatorial plane and they contribute to the network formation, while the other two equatorial oxygen atoms come from the same VP ion (Fig. 1b). The oxygen from the water molecules is situated in the axial plane, because this oxygen is not involved in the network formation and an oxygen atom from a VP ion is also placed in the axial position.

The vinyl groups from VP ions will contribute to the formation of the hydrophobic part of the bidimensional network. Free oxygen atoms of VP ions will connect two  $\text{Ni}^{2+}$  ion neighbors and contribute to network formation. In this way one can link two  $[\text{Ni}_2(\text{VP})_6 \cdot 2\text{H}_2\text{O}]^{8-}$  units (Fig. 1c), or three  $[\text{Ni}_3(\text{VP})_8 \cdot 3\text{H}_2\text{O}]^{10-}$  units. Similarly one can construct models for:  $[\text{Ni}_4(\text{VP})_8 \cdot 4\text{H}_2\text{O}]^{10-}$ ;  $[\text{Ni}_5(\text{VP})_{12} \cdot 5\text{H}_2\text{O}]^{14-}$ ;  $[\text{Ni}_6(\text{VP})_{12} \cdot 6\text{H}_2\text{O}]^{12-}$ ;  $[\text{Ni}_7(\text{VP})_{14} \cdot 7\text{H}_2\text{O}]^{14-}$ ;  $[\text{Ni}_9(\text{VP})_{16} \cdot 9\text{H}_2\text{O}]^{14-}$ . The nine units linked  $[\text{Ni}_9(\text{VP})_{16} \cdot 9\text{H}_2\text{O}]^{14-}$  can present all the elements of an infinite supramolecular network in which one can clearly notice the formation of channels, predicting various practical applications (Fig. 2). In such networks four VP ligands that coordinate a  $\text{Ni}^{2+}$  ion are also bound to four neighboring  $\text{Ni}^{2+}$  ions. For an infinite dimensional network of  $\text{Ni}^{2+}$  it can be mathematically demonstrated that quantitatively to each  $\text{Ni}^{2+}$  ion corresponds only one VP ligand in accordance with TG experimental analysis and with equimolecular mixture of Ni salt and VP acid used in the synthesis. From the synthesis is formed a single compound.

*Demonstration:* By induction in the range of complexes ( $[\text{Ni}(\text{VP})_4 \cdot \text{H}_2\text{O}]^{6-}$ ;  $[\text{Ni}_2(\text{VP})_6 \cdot 2\text{H}_2\text{O}]^{8-}$ ;  $[\text{Ni}_3(\text{VP})_8 \cdot 3\text{H}_2\text{O}]^{10-}$ ;  $[\text{Ni}_4(\text{VP})_8 \cdot 4\text{H}_2\text{O}]^{10-}$ ;  $[\text{Ni}_5(\text{VP})_{12} \cdot 5\text{H}_2\text{O}]^{14-}$ ;  $[\text{Ni}_6(\text{VP})_{12} \cdot 6\text{H}_2\text{O}]^{12-}$ ;  $[\text{Ni}_7(\text{VP})_{14} \cdot 7\text{H}_2\text{O}]^{14-}$ ;  $[\text{Ni}_9(\text{VP})_{16} \cdot 9\text{H}_2\text{O}]^{14-}$ ) we

deduced the basic relationship that can be used to build the network. If we denote by  $n$  the number of  $\text{Ni}^{2+}$  ions from a network line and  $k$  the number of lines in the network, then the total ion  $\text{Ni}^{2+}$  within the network is  $n \cdot k$  and the number of VP ions is  $(n + 1) \cdot (k + 1)$ . This means that on average for each  $\text{Ni}^{2+}$  ion there are  $(n + 1) \cdot (k + 1) / n \cdot k$  VP ions. If the network becomes large, and the number of ions and lines tends to infinity we have the relationship:

$$\lim_{(n \rightarrow \infty; k \rightarrow \infty)} [n + 1] \cdot (k + 1) / n \cdot k = 1$$

Value 1 of this limit explains the thermal analysis result where for each  $\text{Ni}^{2+}$  ion, one VP ion was obtained, proving also why for the synthesis of the compound can be used an equimolar mixture of nickel salt and vinylphosphonate.<sup>22</sup> This means that the four VP ligands who coordinate a  $\text{Ni}^{2+}$  ion are also bind to four neighbors  $\text{Ni}^{2+}$  ions, who leads to the formation of infinite dimensional supramolecular network. Therefore, the network model  $[\text{Ni}_9(\text{VP})_{16} \cdot 9\text{H}_2\text{O}]^{14-}$  is sufficient for quantum-chemical calculations.

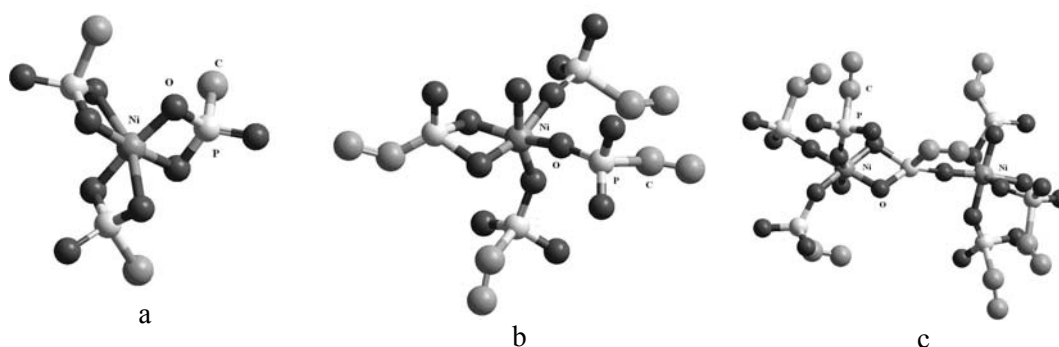


Fig. 1 – The TriVP-Ni (a), TetraVP-Ni (b) and VP-2Ni (c) models representation, O atoms are represented with black color, P atoms with lightgrey and C atoms are represented with grey.

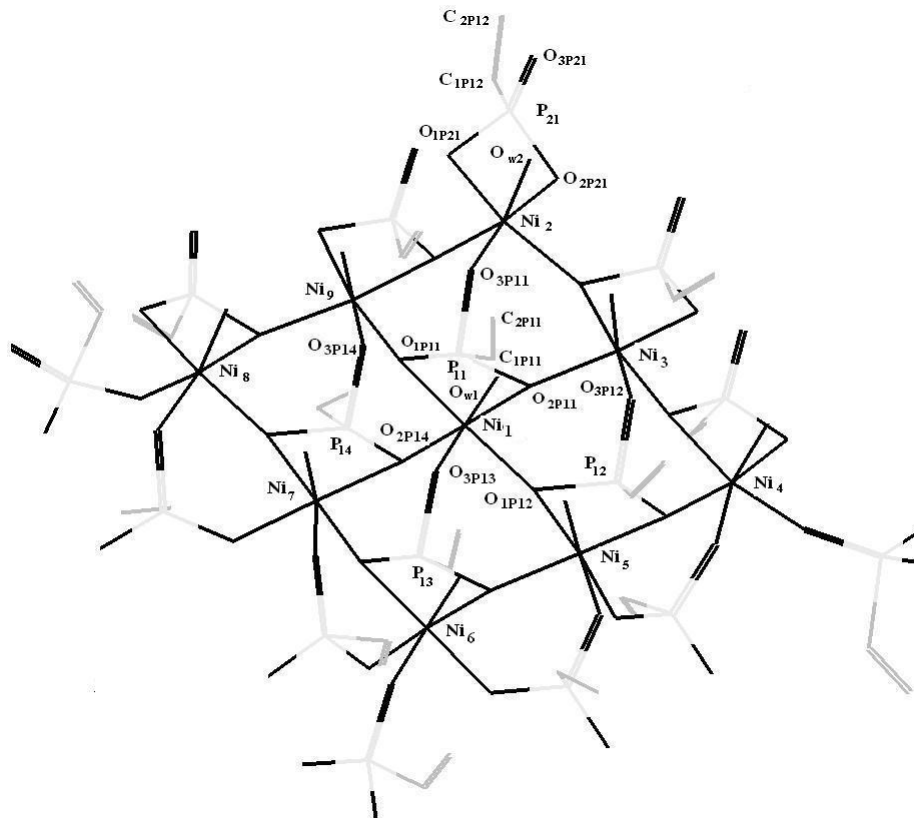


Fig. 2 –  $[\text{Ni}_9(\text{O}_3\text{PCH}=\text{CH}_2)_{16} \cdot 9\text{H}_2\text{O}]^{14-}$  atom numbering. For simplification only the atoms attached to the  $\text{Ni}^{2+}$  central ion and the one attached to an exterior  $\text{Ni}^{2+}$  ion were numbered. The hydrogen atoms were omitted for clarity.

The atom numbering is shown in Fig. 2 for the most complex model VP-9Ni. From Fig. 2 it can be seen that VP-9Ni model presents a 3x3 Ni<sup>2+</sup> squared structure. In order to have a unitary numbering for each model we used the following rule: the central Ni atom is numbered as Ni<sub>1</sub>. The following nickel ions are numbered in clockwise direction. The phosphorus atoms from vinylphosphonates are numbered with P<sub>nickel number phosphorus atom number</sub> (ex. P<sub>11</sub>). The P atoms attached to central nickel ion are all considered as belonging to the central ion and are numbering in the clockwise direction. The other phosphorus atoms are numbered starting for the attached the Ni<sup>2+</sup>. The water oxygen atoms are numbered as O<sub>w nickel number</sub> (ex O<sub>w1</sub> attached to Ni<sub>1</sub>). Oxygen atoms attached to phosphorus are numbered as O<sub>oxygen atom number P nickel number</sub> (ex. O<sub>1P11</sub>). The carbon atoms are numbered in a similar way as oxygen atoms.

In Table 1 the bond lengths for the proposed models in comparison with the experimental results are presented. From Ni<sub>1</sub>-O<sub>w1</sub> and Ni<sub>1</sub>-O<sub>3P13</sub> axial bonds the lengths are with 14% shorter than experimental values. For equatorial oxygen atoms belonging to the same phosphorus atom the calculated and the experimental data are similar.

The calculated values for P-O and P-C bonds are higher than the experimental X-ray data for the central ion. Experimental values for P-O and P-C bonds of 1.54 and 1.79 Å, respectively, are in accordance with the measured values for the outer phosphonate ion. The calculated C=C bond length is similar with the experimental X-ray data being around 1.32 Å.

The calculated bond angles for the axial and equatorial oxygen atoms attached to the central ion are similar with the experimental X-ray data (Table 2). For the oxygen atoms attached to the phosphorus atom (P<sub>11</sub>) coming from the constructed molecules, the angles are higher than the experimental X-ray data. From the VP-7Ni and VP-9Ni the angles are similar or with around 15% smaller.

Torsion angles are similar with the experimental X-ray data (Table 3).

The negative formation heat for the studied compounds in comparison with the heat of

formation of Ni<sup>2+</sup> ion (76.913 kcal/mol) are presented in Table 4 and these values prove the strong tendency of metal organic framework formation. The positive value for VP-2Ni suggests that this model has a low tendency to be formed.

The LUMO-HOMO energetic difference of compounds range from 8.683 eV to 4.899 eV. By increasing the number of nickel atoms in the network it was observed that there is no difference in the LUMO-HOMO energetic differences. The fact that the number of nickel ions does not affect these differences explains the dielectric proprieties of Ni<sup>2+</sup>vinylphosphonate.

Comparing with Co<sup>2+</sup>vinylphosphonate HOMO-LUMO gap (1.465 eV) calculated with PM3 semiempirical method, the cobalt complex displays in its orbital distribution a semi-occupied level, responsible for the semi-conductive property.<sup>23</sup> Ni<sup>2+</sup>vinylphosphonate has a even electrons number occupying all levels, leading to a dielectric behavior justified by the HOMO-LUMO gap (4.995 eV). In Fig. 3 one notes that the levels tend to form a conduction band (LUMO) and the electrons are situated into the occupied levels (HOMO). This difference can explain the dielectric properties of VP-9Ni metal organic network (Fig. 3).

Current measurements for each voltage value have indicated a very low conductivity typical for dielectric materials. Future measurements will follow for determination of dielectric loss tangent.<sup>24</sup>

From the orbital analysis it can be observed that the highest occupied levels are positive and the lowest occupied levels are negative. For each model the first negative levels are 26 for TriVP-Ni, 31 for TetraVP-Ni, 34 for VP-2Ni, 63 for VP-7Ni and 77 for VP-9Ni.

From the orbital components analysis (Fig. 4) it can be observed that from TetraVP-Ni, VP-2Ni and VP-9Ni models in HOMO level are involved  $\sigma$  bonds of the organic functionalities. The *d* orbitals are implied in HOMO level in case of TriVP-Ni and VP-7Ni models.

The orbital analysis suggests that *d* orbitals of Ni<sup>2+</sup> ions are involved in chemical bonds at different levels (Fig. 5).

Table 1

Bond length for central Ni<sup>2+</sup> ion and attached vinylphosphonate atoms

Model/ Bond length	Ni <sub>1</sub> -O <sub>w1</sub>	Ni <sub>1</sub> -O <sub>1P11</sub>	Ni <sub>1</sub> -O <sub>2P11</sub>	Ni <sub>1</sub> -O <sub>1P12</sub>	Ni <sub>1</sub> -O <sub>3P13</sub>	Ni <sub>1</sub> -O <sub>2P14</sub>	P <sub>11</sub> -O <sub>1P11</sub>	P <sub>11</sub> -O <sub>2P11</sub>	P <sub>11</sub> -O <sub>3P11</sub>	P <sub>11</sub> -C <sub>1P11</sub>
TriVP-Ni	-	1.90	1.90	2.05	1.86	1.86	1.55	1.64	1.90	1.93
TetraVP-Ni	1.88	1.84	1.83	1.90	1.93	1.84	1.77	1.80	1.61	1.60
VP-2Ni	1.89	1.84	1.82	1.91	1.98	1.84	1.57	1.55	1.74	1.95
VP-7Ni	1.88	1.86	1.92	1.89	1.87	1.91	1.69	1.98	1.78	2.04
VP-9Ni	1.91	1.90	1.97	2.00	1.86	1.93	1.79	2.12	1.78	1.96
X-ray	2.23	2.24	2.00	2.00	2.24	2.05	1.53	1.53	1.54	1.79

Table 2

Bond angles for central Ni<sup>2+</sup> ion and attached vinylphosphonate atoms

Model/ Angle	O <sub>1P11</sub> -Ni <sub>1</sub> - O <sub>w1</sub>	O <sub>1P11</sub> -Ni <sub>1</sub> - O <sub>2P11</sub>	O <sub>2P11</sub> -Ni <sub>1</sub> - O <sub>1P12</sub>	O <sub>1P12</sub> -Ni <sub>1</sub> - O <sub>2P14</sub>	O <sub>2P14</sub> -Ni <sub>1</sub> - O <sub>1P11</sub>	O <sub>3P14</sub> -Ni <sub>1</sub> - O <sub>w1</sub>	O <sub>1P11</sub> -P <sub>11</sub> - O <sub>3P11</sub>	O <sub>2P11</sub> -P <sub>11</sub> - O <sub>3P11</sub>	O <sub>3P11</sub> -P <sub>11</sub> - O <sub>1P11</sub>	O <sub>1P11</sub> -P <sub>11</sub> - C <sub>1P11</sub>	Ni <sub>1</sub> -O <sub>2P11</sub> - Ni <sub>3</sub>
TriVP-Ni	-	83	92	92	75	-	119	100	119	107	-
TetraVP-Ni	91	76	96	90	90	165	109	109	78	103	-
VP-2Ni	84	73	93	88	94	165	118	111	108	106	-
VP-7Ni	88	85	92	85	96	167	98	109	87	95	135
VP-9Ni	82	92	82	92	90	166	91	108	90	97	137
X-ray	93	86	90	93	87	173	108	108	109	109	123

Table 3

Torsion angles for central Ni<sup>2+</sup> ion and attached vinylphosphonate atoms

Model/ Torsion angle	P <sub>13</sub> - O <sub>3P13</sub> - Ni <sub>1</sub> - O <sub>w1</sub>	O <sub>w1</sub> -Ni <sub>1</sub> - O <sub>2P11</sub> -P <sub>11</sub>	O <sub>1P12</sub> - Ni <sub>1</sub> - O <sub>3P11</sub> - P <sub>13</sub>	O <sub>3P13</sub> - Ni <sub>1</sub> - O <sub>2P11</sub> -P <sub>11</sub>	O <sub>w1</sub> - Ni <sub>1</sub> - O <sub>2P14</sub> - Ni <sub>7</sub>	O <sub>3P13</sub> - Ni <sub>1</sub> - O <sub>2P14</sub> - Ni <sub>7</sub>	Ni <sub>7</sub> - O <sub>2P14</sub> - Ni <sub>1</sub> - O <sub>1P11</sub>	O <sub>1P11</sub> - Ni <sub>1</sub> - O <sub>2P11</sub> -P <sub>11</sub>	O <sub>1P12</sub> - Ni <sub>1</sub> - O <sub>2P11</sub> -P <sub>11</sub>	O <sub>2P14</sub> -Ni <sub>1</sub> - O <sub>1P11</sub> -P <sub>11</sub>	P <sub>11</sub> - O <sub>1P11</sub> - Ni <sub>1</sub> - O <sub>2P11</sub>	P <sub>11</sub> - O <sub>2P11</sub> - Ni <sub>1</sub> - O <sub>2P14</sub>	C <sub>1P11</sub> - P <sub>11</sub> - O <sub>2P11</sub> -Ni <sub>1</sub>	C <sub>2P11</sub> - C <sub>1P11</sub> - P <sub>11</sub> -Ni <sub>1</sub>	C <sub>2P11</sub> - C <sub>1P11</sub> - P <sub>11</sub> -O <sub>2P11</sub>
TetraVP-Ni	177	-72	27	118	-	-	-	-20	140	-142	48	-36	-135	136	-132
VP-2Ni	147	-80	18	93	-	-	-	-9	175	-150	69	-61	-102	106	-156
VP-7Ni	153	-107	24	112	177	-9	84	-8	170	-167	55	-37	-142	89	-138
VP-9Ni	114	-113	34	96	163	-18	79	-28	167	-157	33	-91	-96	139	-135
X-ray	180	-92	52	84	161	-12	74	-3	174	-174	49	-49	-110	120	-120

Table 4

Calculated electronic and thermodynamic properties

Model/Electronic properties	$\Delta H_{\text{form}}$	ZPE	HOMO	LUMO	LUMO-HOMO
TriVP-Ni	-388.93	92.18	6.914	15.597	8.683
TetraVP-Ni	-121.08	149.84	11.508	17.142	5.634
VP-2Ni	229.24	266.62	17.166	22.105	4.939
VP-7Ni	-1134.04	614.17	19.352	24.251	4.899
VP-9Ni	-2206.97	726.71	19.150	24.148	4.998

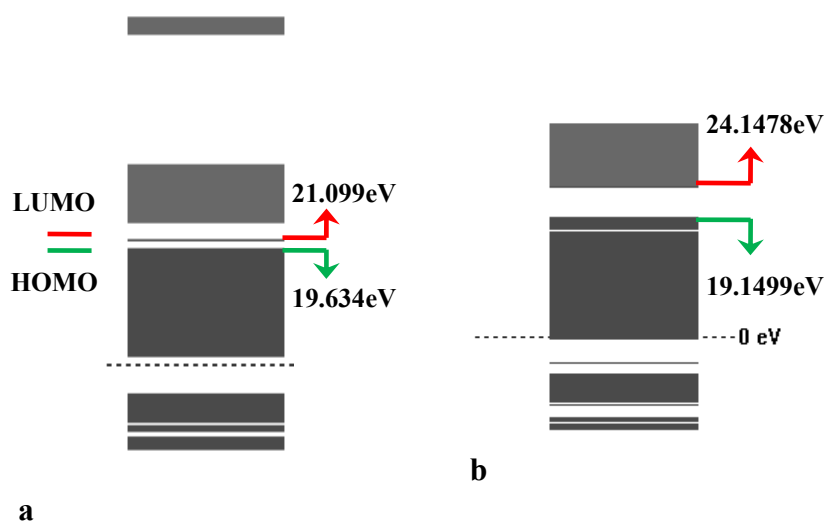


Fig. 3 – Representation of the VP-9Co (a) and VP-9Ni (b) orbital distributions.

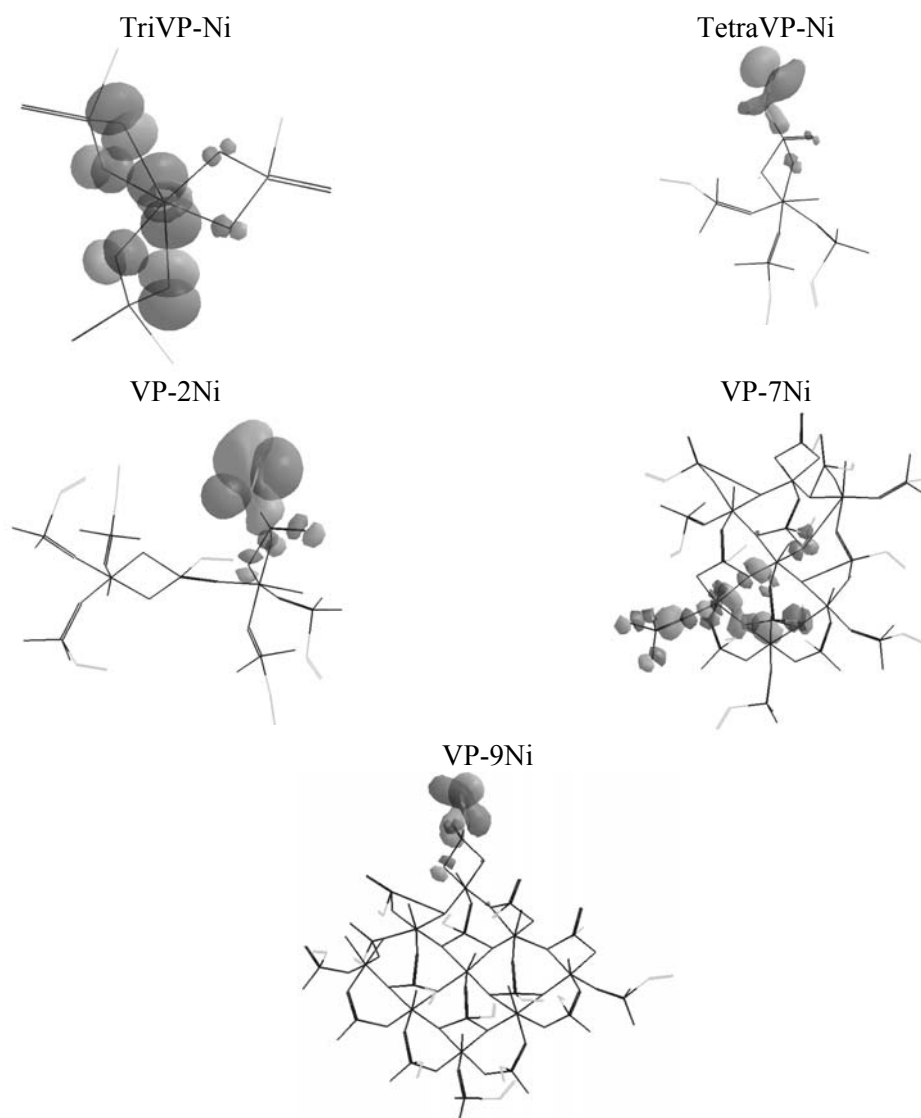


Fig. 4 – The HOMO orbital components.

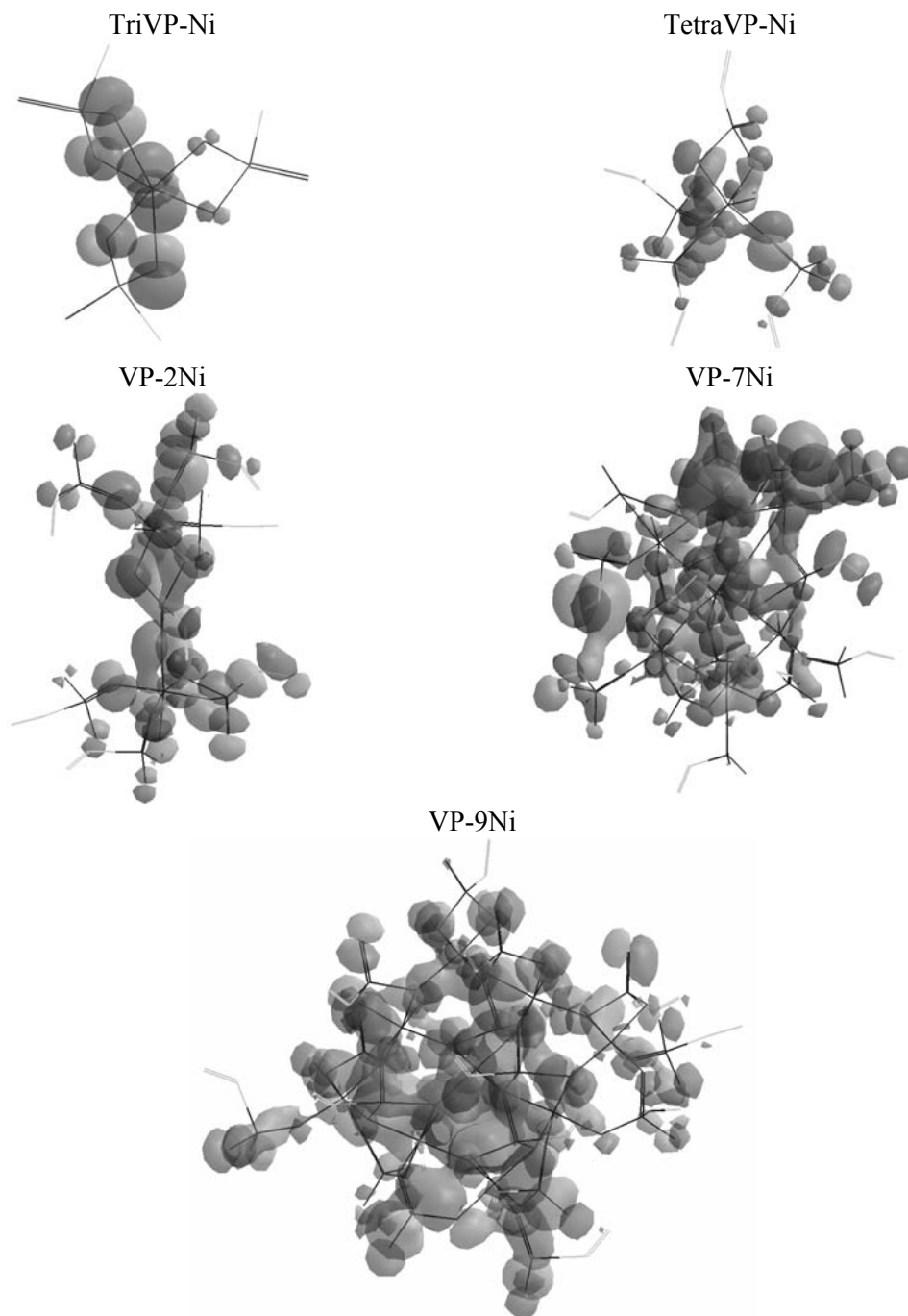


Fig. 5 – First energetic level in which the  $\text{Ni}^{2+}$  central ion have implied a d orbital.

### CONCLUSION

The analysis of the geometrical data by PM3 semi-empirical method gives shorter bond lengths than the experimental data. The bond angles are similar or higher comparing with the experimental values and torsion angles are comparable with the experimental X-ray data.

The d orbitals are implied in HOMO level in case of TriVP-Ni and VP-7Ni models. For all the

other models in HOMO level are involved  $\sigma$  bonds of the organic functionalities.

The calculated thermodynamic data explains the metal organic network formation tendency.

Electric conductivity measurements indicate the  $\text{Ni}^{2+}$  vinylphosphonate as dielectric while the corresponding  $\text{Co}^{2+}$  vinylphosphonate is a semiconductor. This agrees with the calculated LUMO-HOMO energetic difference of 4.997 eV

for Ni<sup>2+</sup> vinylphosphonate and 1.465 eV for Co<sup>2+</sup> vinylphosphonate.

In this work for the first time in literature a mathematical relationship which demonstrates the formation of an infinite dimensional network of Ni<sup>2+</sup> with phosphonates was deduced.

*Acknowledgments:* The authors thank to the National Council for Research and High Education (CNCSIS) for allowing the financial backgrounds use for purchasing the HyperChem 7.52 package by CNCSIS grant no.776/2005/Agreement 27658/2005/GR177/ 2006/1973/2006. Research was partially supported by Program no 2, Project no. 2.4 from the Institute of Chemistry Timisoara of Roumanian Academy.

## REFERENCES

1. A.K. Cheetham, C.N.R. Rao and K. Feller, *Chem. Commun.*, **2006**, 46, 4780-4795.
2. S. Kitagawa and K. Uemura, *Chem. Soc. Rev.*, **2005**, 34, 109-119.
3. T.K. Maji and S. Kitagawa, *Pure. Appl. Chem.*, **2007**, 79, 2155-2177.
4. A.K. Bar, R. Chakrabarty, G. Mostafa, and Mukherjee, *Angew. Chem., Int. Ed.* **2008**, 47, 8455-8459.
5. J.L.C. Rowsell and O.M. Yaghi, *Angew. Chem., Int. Ed.*, **2005**, 47, 4670-4679.
6. S. Ma, D. Sun, M. Ambrogio, J.A. Fillinger, S. Parkin and H.C. Zhou, *J. Am. Chem. Soc.*, **2007**, 129, 1858-1859.
7. S. Ma, D. Sun, J.M. Simmons, C.D. Collier, D. Yuan and H.C. Zhou, *J. Am. Chem. Soc.*, **2008**, 130, 1012-1016.
8. N. Guillou, P.M. Forster, Q. Gao, J.S. Chang, M. Nogues, S.E. Park, A.K. Cheetham and G. Férey, *Angew. Chem., Int. Ed.*, **2001**, 40, 2831-2834.
9. J.S. Seo, D. Whang, H. Lee, S.I. Jun, J. Oh, Y.J. Jeon and K. Kim, *Nature*, **2000**, 404, 982-986.
10. G. Li, W. Yu, J. Ni, T. Liu, Y. Liu, E. Sheng and Y. Cui, *Angew. Chem., Int. Ed.*, **2008**, 47, 1245-1249.
11. B. Chen, Y. Ji, M. Xue, F.R. Fronczek, E.J. Hurtado, J.U. Mondal, C. Liang and S. Dai, *Inorg. Chem.*, **2008**, 47, 5543-5545.
12. B.C. Tzeng, T.H. Chiu, B.S. Chen and G.H. Lee, *Chem. Eur. J.*, **2008**, 14, 5237-5245.
13. H.C. Yao, Y.Z. Li, S. Gao, Y. Song, L.M. Zheng and X.Q. Xin, *J. Solid State Chem.*, **2004**, 177, 4557-4563.
14. G. Alberti, F. Cherubini and R. Palombari, *Sensors Actuators B: Chem.*, **1995**, 24, 270-272.
15. E.W. Stein, A. Clearfield and M.A. Subramanian, *Solid State Ionics*, **1996**, 83, 113-124.
16. G. Ilia, S. Iliescu, L. Macarie, B. Maranescu and A. Pascariu, *ROMPHYSICHEM-12*, Bucharest, Roumania, September 6-8, **2006**, 198.
17. A. Cabeza, R.M.P. Colodrelo, L. Leon-Reina, M.A.G. Aranda, K.D. Demadis and G. Ilia, *11<sup>th</sup> European Powder Diffraction Conference*, Warsaw, Poland, 19-22 September **2008**, 57.
18. R.M.P. Colodrero, A. Cabeza, P. Olivera-Pastor, D. Choquesillo-Lazarte, A. Turner, G. Ilia, B. Maranescu, K. E. Papatthaniou, G.B. Hix, K.D. Demadis, M.A.G. Aranda, *Inorg. Chem.*, **2011**, 50, 11202-11211.
19. a) M.J.S. Dewar, E.G. Zuebisch, E.F. Healy and J.J.P. Stewart, *J. Am. Chem. Soc.*, **1985**, 107, 3902-3909; b) J.J.P. Stewart, *J. Comput. Chem.*, **1989**, 10, 209-220, 221-264; c) J.J.P. Stewart, *J. Comput. Chem.*, **1991**, 12, 320-334; d) J.J.P. Stewart, *J. Mol. Model.*, **2004**, 10, 155-164.
20. I.N. Levine, "Quantum Chemistry", 5th Edition, Prentice Hall, Inc., Upper Saddle River, New Jersey 07458 2000, Chap. 15, Chap. 17.
21. \*\*\* HyperChemTM, Release 7.52 for Windows, Copyright **2003**, Hypercube, Inc, 1115 NW 4th Street, Gainesville, FL 32601, US.
22. Supplementary materials, see on:
23. B. Maranescu, A. Visa, M. Mracec, G. Ilia, V. Maranescu, Z. Simon and M. Mracec *Rev. Roum. Chim.*, **2011**, 56, 473-482.
24. V. Maranescu, A. Visa, M. Mracec, B. Maranescu, G. Ilia, T. Oprea and M. Mracec, **2011**, unpublished results.